

AD-A015 716

EFFECTS OF TEMPERATURE ON THE KINETICS OF PASSIVE
FILM GROWTH ON IRON

C. N. Lukac, et al

Ohio State University

Prepared for:

Office of Naval Research

September 1975

DISTRIBUTED BY:

NTIS

National Technical Information Service
U. S. DEPARTMENT OF COMMERCE

UNCLASSIFIED

SECURITY CLASSIFICATION OF THIS PAGE (When Data Entered)

REPORT DOCUMENTATION PAGE		READ INSTRUCTIONS BEFORE COMPLETING FORM
1. REPORT NUMBER	2. GOVT ACCESSION NO.	3. RECIPIENT'S CATALOG NUMBER
4. TITLE (and Subtitle) EFFECTS OF TEMPERATURE ON THE KINETICS OF PASSIVE FILM GROWTH ON IRON		5. TYPE OF REPORT & PERIOD COVERED Technical Report 1 March '74 to 28 Feb. '75
7. AUTHOR(s) C.N. Lukac, J.B. Lumsden, Z. Smialowska, and R.W. Staehle		6. PERFORMING ORG. REPORT NUMBER 3003-A1 No. 6
9. PERFORMING ORGANIZATION NAME AND ADDRESS The Ohio State University Research Foundation 1314 Kinnear Road Columbus, Ohio 43212		8. CONTRACT OR GRANT NUMBER(s) N00014-67-A-0232-0006
11. CONTROLLING OFFICE NAME AND ADDRESS Office of Naval Research Department of the Navy Arlington, Virginia 22217		10. PROGRAM ELEMENT, PROJECT, TASK AREA & WORK UNIT NUMBERS NR 036-085 Code 471
14. MONITORING AGENCY NAME & ADDRESS (if different from Controlling Office) Office of Naval Research Resident Representative The Ohio State University Research Center 1314 Kinnear Road Columbus, Ohio 43212		12. REPORT DATE September 1975
16. DISTRIBUTION STATEMENT (of this Report) Reproduction in whole or in part is permitted for any purpose of the United States Government		13. NUMBER OF PAGES 45
17. DISTRIBUTION STATEMENT (of the abstract entered in Block 20, if different from Report)		15. SECURITY CLASS. (of this report) UNCLASSIFIED
18. SUPPLEMENTARY NOTES This work has been accepted for publication by THE JOURNAL OF THE ELECTROCHEMICAL SOCIETY.		15a. DECLASSIFICATION/DOWNGRADING SCHEDULE
19. KEY WORDS (Continue on reverse side if necessary and identify by block number) Corrosion Passivity Iron Films Ellipsometry		
20. ABSTRACT (Continue on reverse side if necessary and identify by block number) Ellipsometry was used to investigate the effects of temperature and potential on the growth kinetics of passive films on iron exposed to a pH 8.6 borate buffer solution. It was found that over the temperature range of 0-80°C the growth kinetics could be described with an equal degree of confidence by either logarithmic, inverse logarithmic, or a modified form of inverse logarithmic kinetics. None of the existing models for film growth were found to be completely consistent with the temperature and potential dependencies of the growth constants.		

DD FORM 1473

1 JAN 73

EDITION OF 1 NOV 65 IS OBSOLETE

UNCLASSIFIED

SECURITY CLASSIFICATION OF THIS PAGE (When Data Entered)

EFFECTS OF TEMPERATURE ON THE KINETICS
OF PASSIVE FILM GROWTH ON IRON*

by
C.N. Lukac, J.B. Lumsden, Z. Smialowska, and R.W. Staehle

Sixth Technical Report to
Office of Naval Research
Contract N00014-67-A-0232-0006, NR 026-085
1 March 1974 to 28 February 1975

"Fundamental Studies of Dissolution and
Passivity of Alloys and Compounds"

The Ohio State University
Department of Metallurgical Engineering
September 1975

Distribution of this document is unlimited.

Reproduction in whole or in part is permitted for any purpose
of the United States Government

*This paper is accepted for publication in THE JOURNAL OF THE
ELECTROCHEMICAL SOCIETY

INTRODUCTION

There have been several ellipsometric studies (1-8) of the passive film formed on iron in near-neutral solutions. These investigations have shown that the film thickness is directly proportional to the applied potential and that film growth can be described equally well by either inverse logarithmic or logarithmic kinetics. Thus, it has not been possible to identify the model which represents the growth of this film from existing results. This investigation was undertaken to assess possible distinguishing features which might corroborate one of the proposed models for film growth. This was approached by measuring the temperature dependence of film thickening.

In order to correlate with the experimental data we review briefly here the four major models for interpreting film growth on metal surfaces. The first of these is the inverse logarithmic model proposed by Mott and Cabrera (9). This model assumes field assisted cation diffusion according to which the potential drop, V , across the film remains constant while the field, V/X , decreases as the film thickens. The rate determining step is assumed to be the surmounting of the potential barrier, W , between the metal-oxide interface. The rate of film growth is given by the expression

$$\frac{dx}{dt} = u_0 \exp (qaV - W)/kT \quad (1)$$

where

$$u_0 = Na^4\nu; \quad (2)$$

N is the number of mobile ions per unit volume of oxide; a is the jump distance; q is the charge on the ion, W is the activation energy; ν is the phonon frequency. If the absolute reaction rate theory is used, $\nu = (kT/h)$. Mott and Cabrera give an approximate integration of equation (1) as

$$1/x = \frac{kT}{qaV} \ln \frac{x_1^2 kT}{qaVu_0} + \frac{W}{qaV} - \frac{kT}{qaV} \ln t \quad (3a)$$

or

$$1/x = A - B \ln t \quad (3b)$$

The quantity, x_1 , is the average film thickness over the range considered.

Recently, Ghez (10) has examined the integration of equation (1).

According to his results the inverse logarithmic kinetic expression derived by Mott and Cabrera is not an asymptotic solution to this equation. His basic objection is the approximation of X by X_1 . He obtains as a solution the expression

$$1/x = \frac{kT}{qaV} \ln \frac{kT}{qaVu_0} + \frac{W'}{qaV} - \frac{kT}{qaV} \ln \frac{t + t_0}{x^2} \quad (4a)$$

or

$$1/x = A' - B' \ln \frac{t + t_0}{x^2} \quad (4b)$$

Sato and Cohen (11) have proposed a model which rationalizes logarithmic kinetics. According to their suggestion, film growth proceeds by the field assisted place-exchange of metal-oxygen pairs. All such pairs in a given row normal to the surface are assumed to exchange places simultaneously.

This model gives a growth rate

$$\frac{dx}{dt} = 2 \alpha(T) \exp \frac{FV}{2RT} - \frac{xW_0}{avRT} \quad (5)$$

which integrates to

$$X = \frac{avRT}{W_0} \ln \frac{W_0 \alpha}{avRT} + \frac{avFV}{2W_0} - \frac{avRT}{W_0} \ln (t_0 + t) \quad (6a)$$

or

$$X = C + D \log (t + t_0) \quad (6b)$$

where a is the lattice constant, v the stoichiometric number, W_0 the chemical potential between a cation in the activated state and the normal state in any lattice layer, and

$$\alpha(T) = \beta T \exp \delta/T \quad (7)$$

Here β and δ are constants independent of potential and temperature.

Fehlner and Mott (12) have described logarithmic growth differently. They suggest that the structure of the film changes with thickness so that the potential drop across the film increases as the film thickens in such a way that the field remains constant. With this assumption the activation energy is of the form $W_0 + \mu x$; therefore,

$$\frac{dx}{dt} = A \exp [-(W_0 + \mu x)/kT] \quad (8)$$

and

$$x = kT/\mu \ln \mu A/kT - W_0/\mu + kT/\mu \ln (t + t_0) \quad (9a)$$

$$x = C + D \log (t + t_0) \quad (9b)$$

In the results reported here we have determined the thickness of the passive films on iron as a function of time, potential and temperature using ellipsometry. The results have been analyzed in terms of the above three models of film growth.

EXPERIMENTAL

A schematic diagram of the cell used is shown in Figure 1. This was a double-walled glass vessel having optically flat pyrex windows and a capacity of 500 ml. The cell consisted of a Luggin capillary leading through a wetted, closed stop-cock to a saturated calomel reference electrode. The temperature of the solution was measured by a thermometer positioned 2 cm from the sample. Temperature control was maintained by circulating ethylene glycol through the jacket. The cell was connected to a double-walled 2 liter reservoir where the electrolyte was deaerated by bubbling with prepurified helium; the temperature of the solution was raised or lowered as desired before it was admitted to the cell.

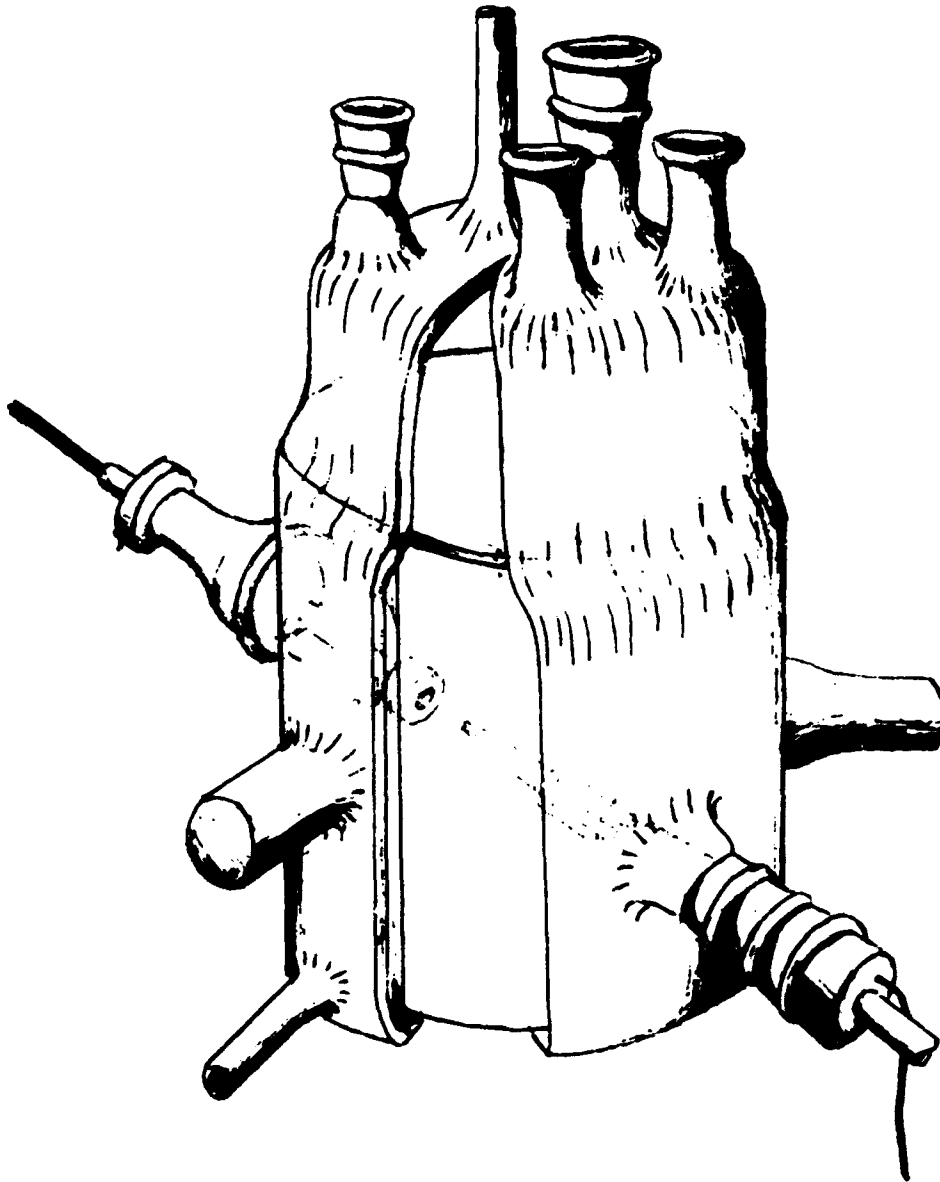


Figure 1. Schematic of the ellipsometric-electrochemical cell.

The iron specimen was a 99.99% zone refined rod with a threaded hole for the electrical connection. It was mounted in a teflon holder and had an exposed area of 0.32 cm^2 .

The solution used was an equivolume mixture of $0.15\text{N H}_3\text{BO}_3$ and $0.15\text{N Na}_2\text{B}_4\text{O}_7$ (pH 8.7). Measurements were made at 0, 20, 35, 50, and 80°C . The solutions were deaerated by bubbling prepurified helium for at least 24 hours.

The ellipsometer was a Rudolph & Sons, Type 43603-200E. A Keithley model 4145 picoammeter was used to measure the output from the photomultiplier tube (RCA 1P21). All measurements were made using the 5461 \AA mercury green line.

Before placing the sample in the cell, it was mechanically polished to a $1/4 \text{ }\mu\text{m}$ finish using diamond paste. The specimen was then cleaned, degreased, and electropolished in a solution consisting of 20 parts glacial acetic acid to one part 20% perchloric acid. Next the sample was washed with double distilled water and then with reagent grade methanol, dried and placed in the cell.

The specimen was first cathodically reduced at a constant current density of $40 \mu\text{A}/\text{cm}^2$. Cathodic reduction was continued until the optical constants of the film-free surface were obtained. The passive film was then formed potentiostatically by switching directly from the cathodic potential (approximately -1.0 V SCE) to the desired potential in the passive region. The sample was polarized approximately one hour at each potential; measurements of the ellipsometric parameters were made at 10 minute intervals. This procedure was repeated 3-5 times at each potential.

The optical constants obtained for the film free surface are in satisfactory agreement with those found by others as shown in Table 1. These values also compare favorably with those measured by Yolken and Kruger (13) for a

film free surface in an ultra-high vacuum.

A cathodic current density of $40\mu\text{A}/\text{cm}^2$ was used to reduce the film since at this current density it could be removed within 10-15 minutes. The final potential attained was close to that established by others (6,7,8) for this system as "the optical reference state".

It was found to be unnecessary to change the solution after cathodic reduction in order to avoid the effects of ferrous ions. Several measurements were made following the procedure of replacing the solution after reduction, excluding oxygen, while maintaining the surface at the reduction potential. The steady state results were the same as those for the unrefreshed solution.

RESULTS

The current-potential curves for iron exposed to the borate buffer solutions with the range of temperatures 0-80°C are shown in Figure 2. These curves were obtained by scanning at a rate of 20 mV/min. There was no measureable change in pH over this temperature range.

The optical constants of the film were determined using the first order approximation of the ratio of the Fresnel reflection coefficients (16). Thus, if the film thickness is less than 50-100 Å, the change in both of the ellipsometric parameters $\delta\Delta$ and $\delta\psi$ is directly proportional to the thickness. This implies that $\delta\Delta$ and $\delta\psi$ are related linearly. The $\delta\Delta$ vs $\delta\psi$ curve for films formed at 20°C is given in Figure 3. This is the least squares curve and was found to be linear at the 95 per cent confidence level by the F ratio test. The standard deviation of the slope was 4.6%. It is not possible to obtain unique values for the optical constants using this curve. This is one of the inherent problems associated with the ellipsometric technique when working with semiconducting films of unknown thicknesses. The difficulty arises

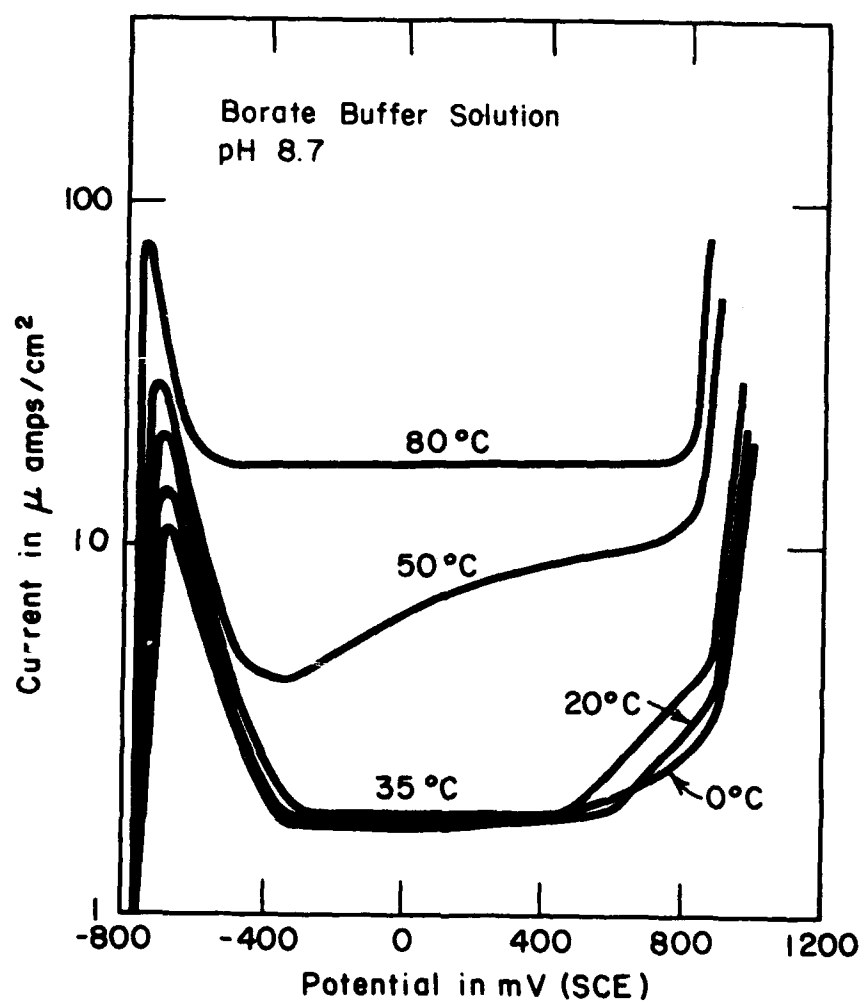


Figure 2. The current density-voltage curves for Fe exposed to a pH 8.7 borate buffer solution at 0°, 20°, 35°, 50°, and 80°C.

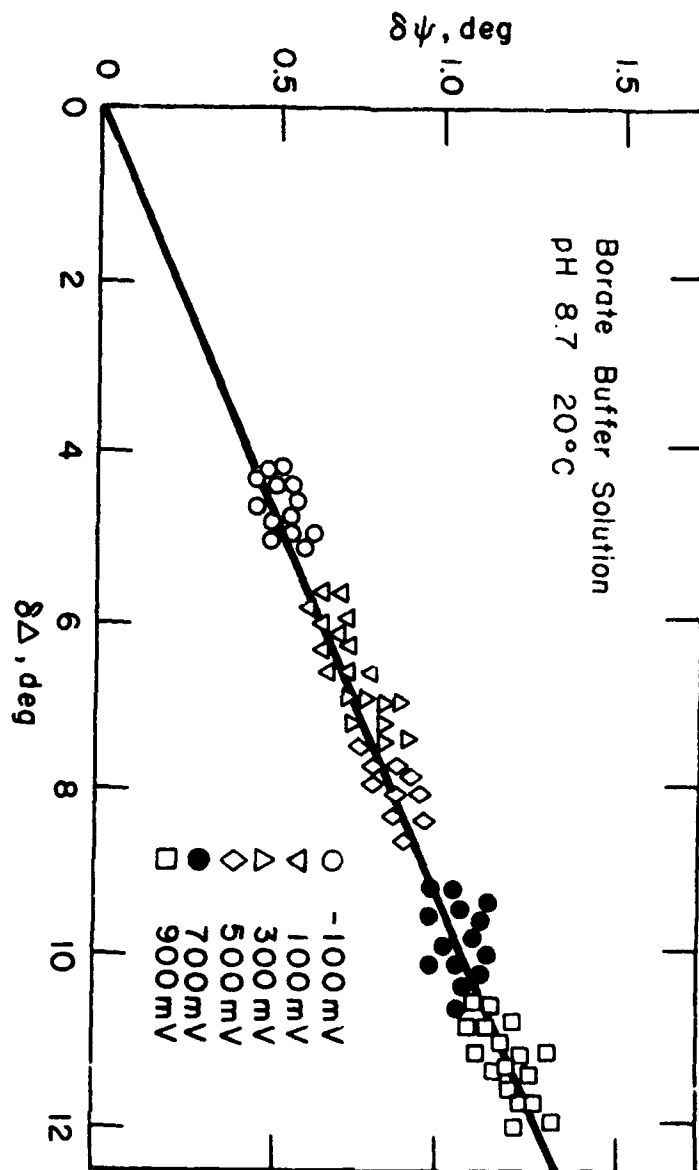


Figure 3. The $\delta\psi$ and $\delta\Delta$ values for the anodic oxidation of Fe in a pH 8.7 borate buffer solution at 20°C.

since there are three unknowns (the thickness, the index of refraction, and the absorption coefficient), and only two experimental parameters, Δ and ψ . Accordingly, the real part of the refractive index was assumed to be 2.6 and the imaginary part was determined by fitting a theoretical curve, which was calculated using the exact equations (17), to the least squares curve. The curve which gave the best fit corresponded to the optical constants $2.6(1-0.19i)$. As shown in Table 1 these optical constants are in good agreement with those rationalized by others at room temperature.

Table 1 Optical Constants of Iron and Iron Oxides

$n_2 = n(1-ik)$		Room Temperature	
Source	Material	n	k
Kruger and Yolren ¹	Fe	3.35	1.15
Ord and Desmet ²	Fe	3.50	1.05
Sato and Kudo ³	Fe	3.18	1.21
Present Work	Fe	3.21 ± 0.02	1.26 ± 0.02
Winterbottom ¹⁴	Fe_3O_4	2.50	0.12
Bockris et.al. ¹⁵	Fe_3O_4	2.39	0.104
Winterbottom	$\alpha-Fe_2O_3$	3.42	0.309
Bockris et.al. ¹⁵	$\gamma-Fe_2O_3$	2.88	0.131
Kruger and Calvert ¹	Anodic Film on Fe (room temperature)	2.50	0.12
Ord and Desmet ²	Anodic Film on Fe (room temperature)	2.60	0.15
Sato and Kudo ³	Anodic Film on Fe (room temperature)	2.55	0.137

The same procedure was used to find the optical constants at each temperature. A minimum of seventy points was used to obtain each curve. The standard deviations in the slope of the $\delta\psi$ vs. $\delta\Delta$ curves ranged from 2.2% for 35° to 7.8% for 80°. The values of the optical constants for each temperature are given in Table 2. All are the same within error except those determined for films formed at 0 and 35°C. The imaginary parts of the optical constants for these films are substantially smaller than those formed at other temperatures.

The least squares curves of the reciprocal of the film thickness vs. $\log t$ and $\log t/x^2$ and the film thickness vs. $\log t$ are shown in Figures 4, 5, and 6. Plots are given as a function of potential for films formed in solutions at 0, 35, 50, and 80°C. Results were also obtained at 20°C but are not shown. Each of these curves were found to be linear well within the 95% confidence level using the F ratio test. The confidence level of the fit was approximately the same for all three models.

Table 3 gives the values of the constants

A, B, A', B', C and D where

$$1/x = A - B \ln t \quad (8)$$

$$1/x = A' - B' \ln t/x^2 \quad (9)$$

and

$$x = C + D \ln t \quad (10)$$

The quantity $1/B$ vs. potential is plotted in Figure 7 and $1/B'$ vs. potential in Figure 8. These show that B and B' are directly proportional to potential and that the proportionality constant, m, (the slope), is temperature dependent. There is some scatter in these results; nevertheless, the least squares analysis indicates that the correlation for the set of

Table 2 Optical Constants of Anodic Film

$$n_2 = n(1 - ik)$$

Temperature °C	n	k
0	2.60	0.04
20	2.60	0.19
35	2.60	0.07
50	2.60	0.20
80	2.60	0.20

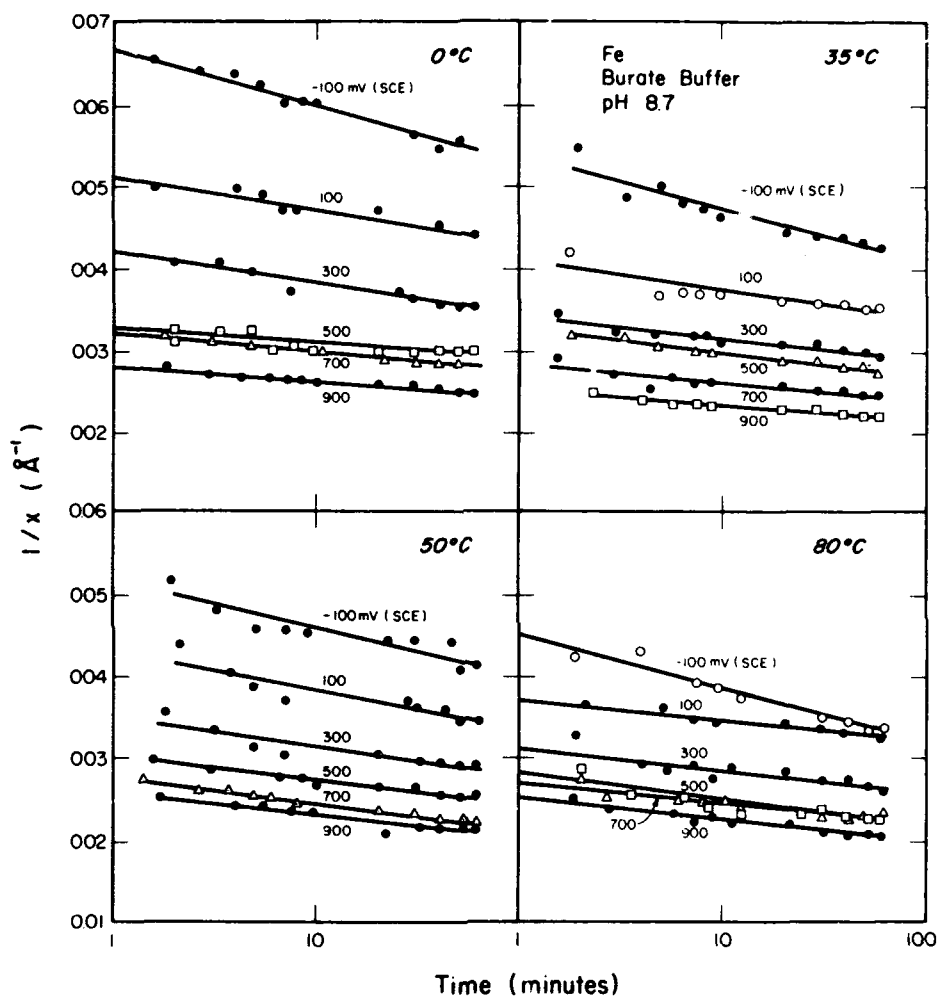


Figure 4. The reciprocal of film thickness vs. log of time as a function of temperature and potential.

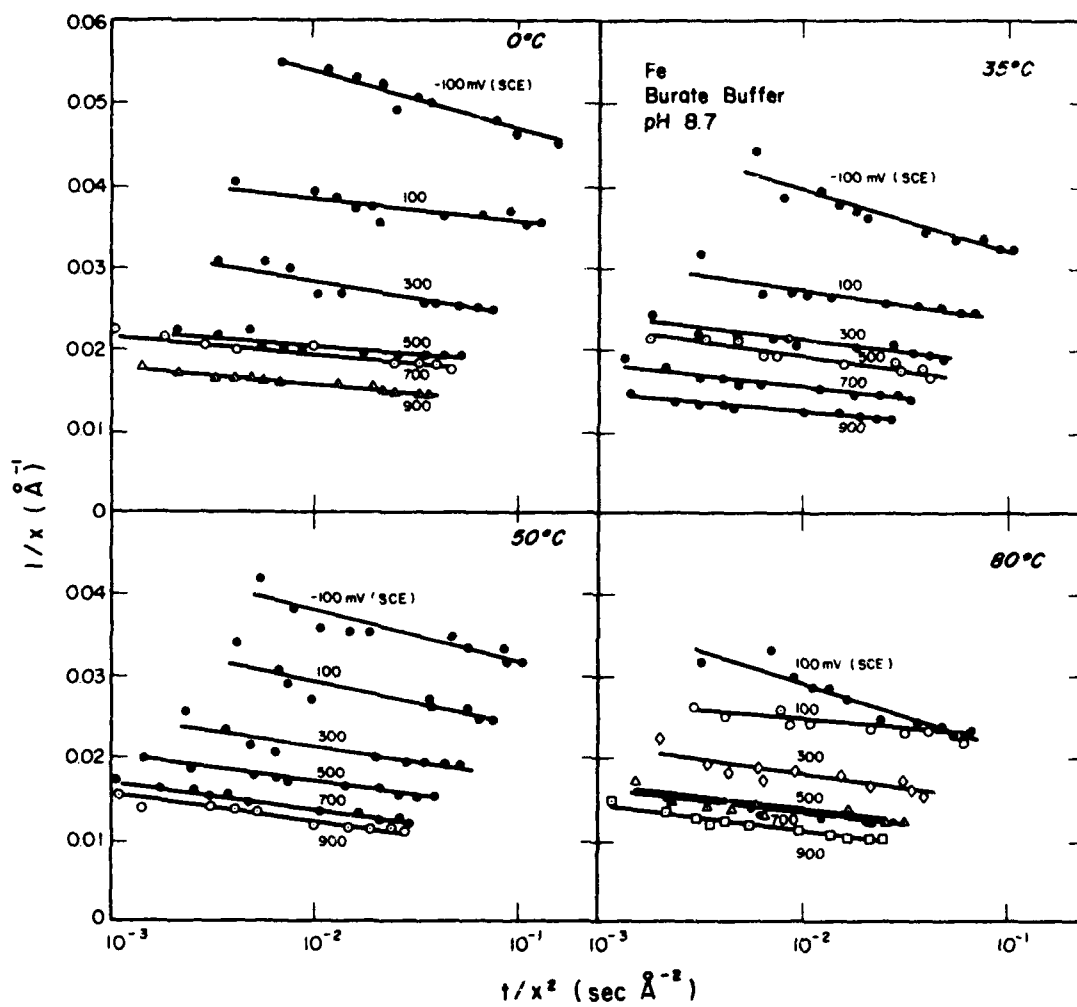


Figure 5. The reciprocal of film thickness vs. log of time divided by the film thickness squared.

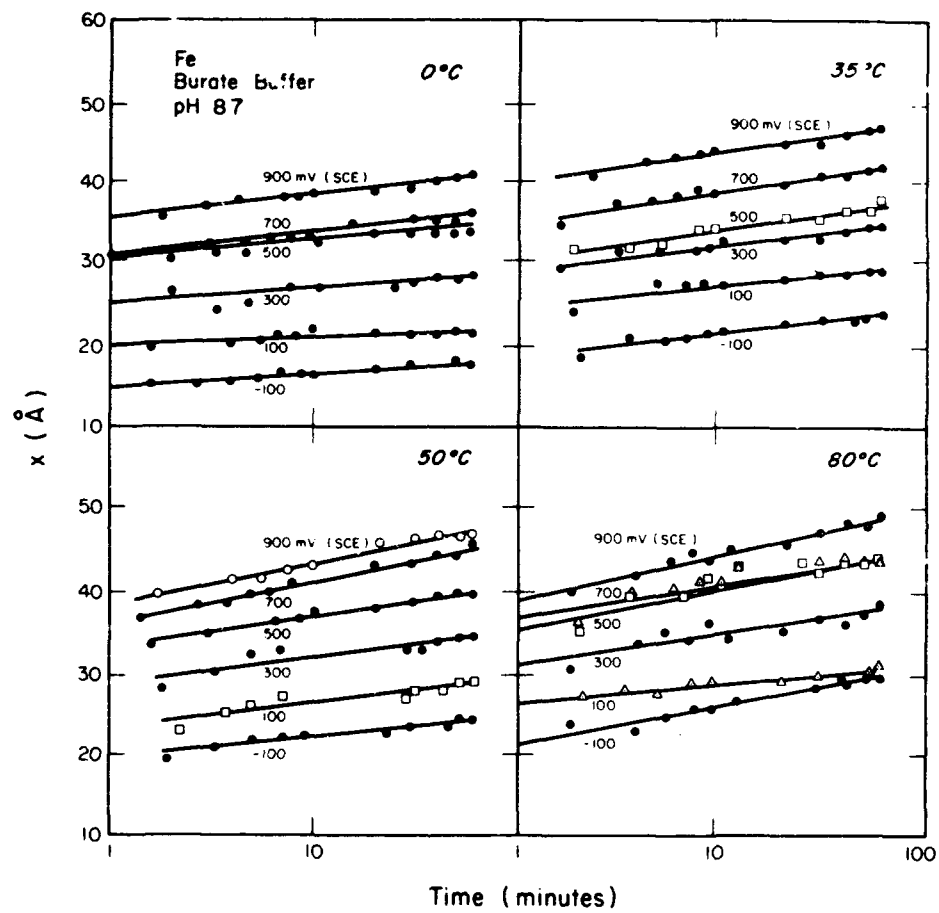


Figure 6. Logarithmic plot showing the changes in the thickness of the passive film on iron with time.

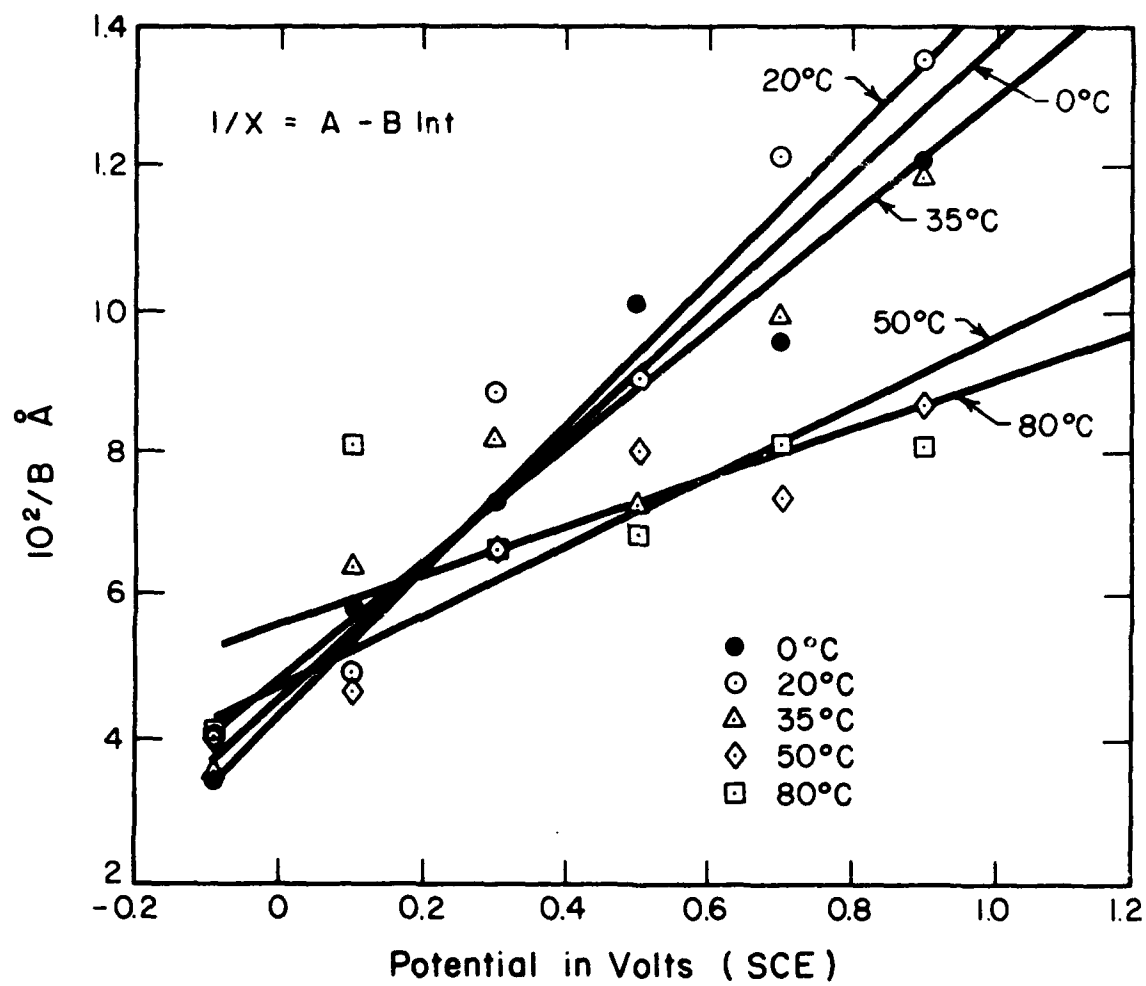


Figure 7. The reciprocal of the rate constant B vs. applied potential.

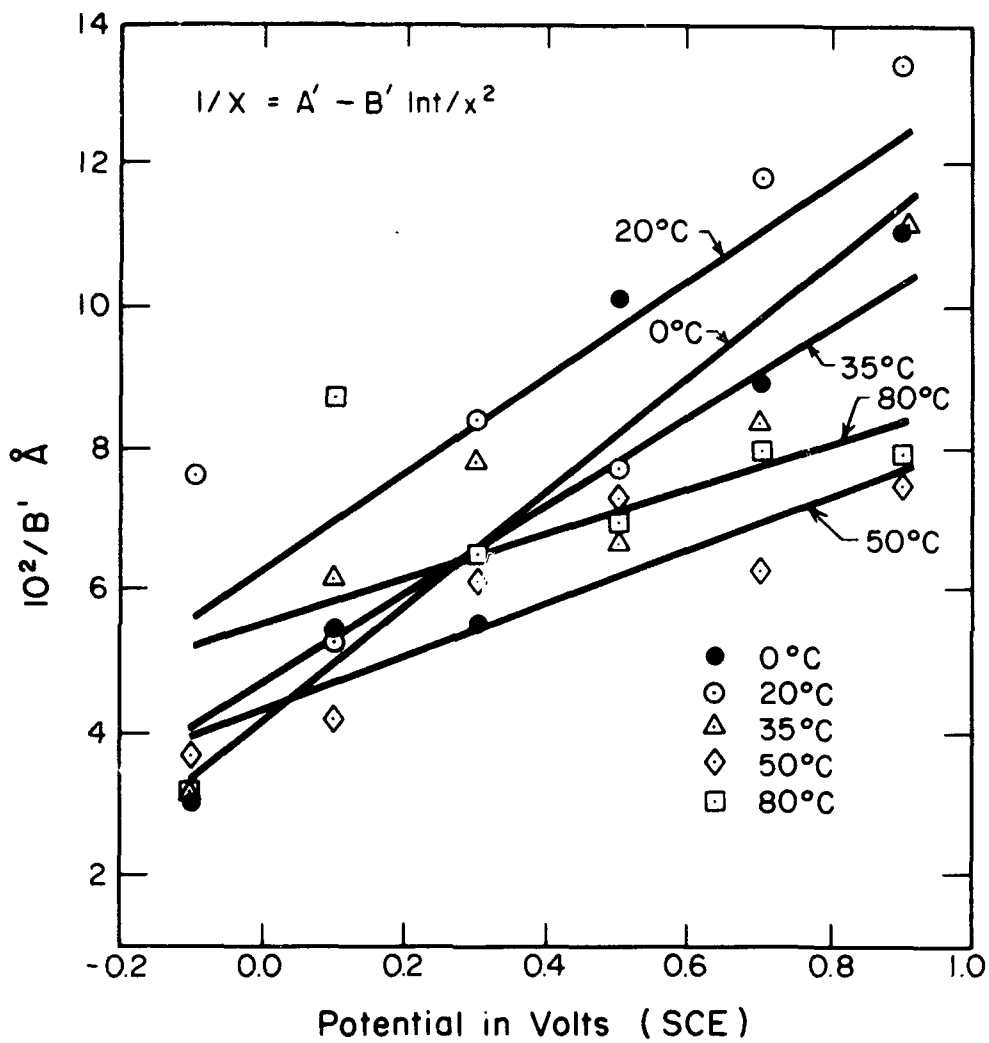


Figure 8. The reciprocal of the rate constant B' vs. applied potential.

data for each temperature is linear at the 95 per cent confidence level.

The results of Figure 9 show the slopes of the curves in Figure 7 and 8, m_1 . A least squares analysis of the data gives a linear relationship. This is in accordance with equations 3 and 4, i.e.,

$$B = B' = kT/qaV \quad (10)$$

These correlations show that B and B' are inversely proportional to V and directly proportional to T in agreement with the Mott-Cabrera model.

It should be pointed out that the applied electrochemical potential, which is that given in Figures 7 and 8, is not the potential drop, V, across the film. However, it differs from V only by an additive constant. Thus, the only effect of plotting the electrochemical potential instead of V is a shift in the axis. This assumes that the potential across the double layer remains constant.

The jump distance, a, was calculated using the slopes in Figure 7 and 8 since $m_1 = kT/qa$. These values are given in Table 4. Figure 10 shows that the jump distance as determined using inverse logarithmic kinetics as well as a' from the modified inverse logarithmic kinetic model decreases linearly with temperature.

Figure 11 and 12 show that A and A' are linearly related to the inverse of the potential with a temperature dependent slope, m_2 . This potential dependence is in accordance with equations 3a and 4a since $\ln \frac{x_1^{2kT}}{qaVu^0}$ is a slowly varying function of T and V over the ranges considered. The temperature dependence of the slopes, m_2 , is shown to be linearly related to the temperature in Figure 13. This indicates that A and A' are directly proportional to the temperature.

The constant D appears to behave in a random fashion with potential;

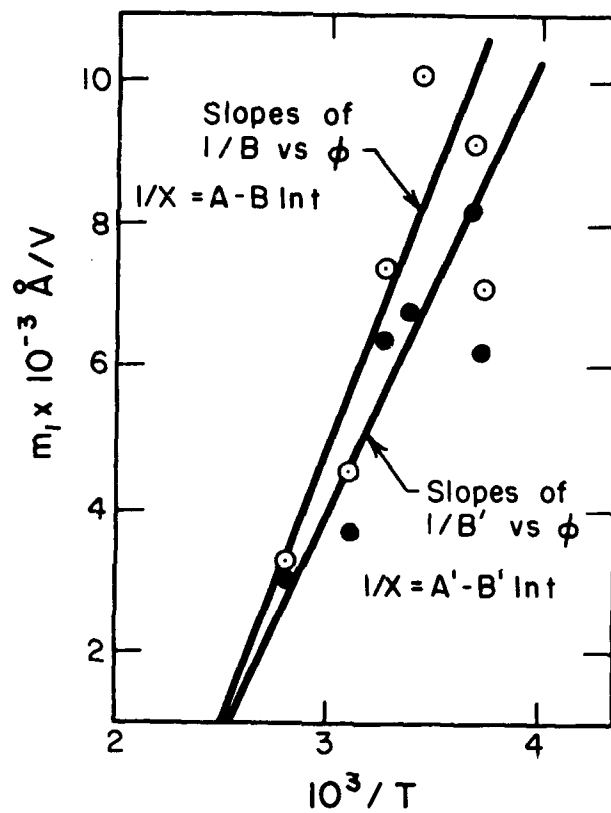


Figure 9. The relationship between the reciprocal of temperature and the slopes of the $1/B$ and $1/B'$ vs. applied potential curves.

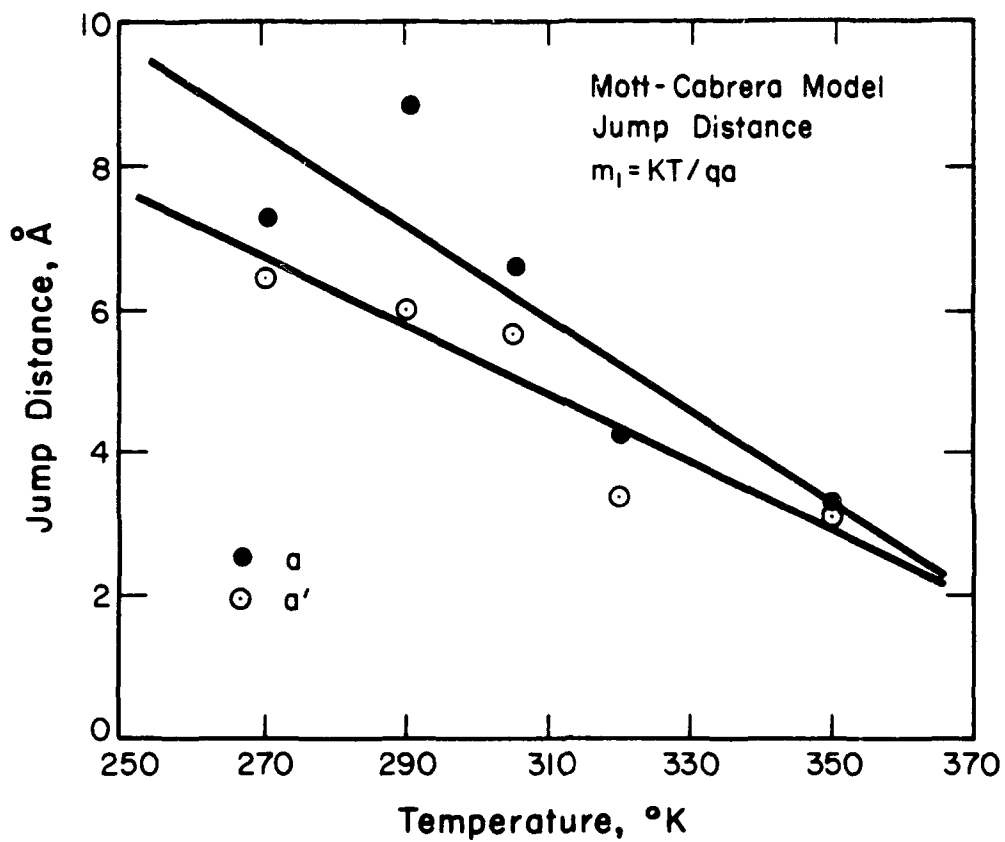


Figure 10. The values of the jump distance as a function of temperature.

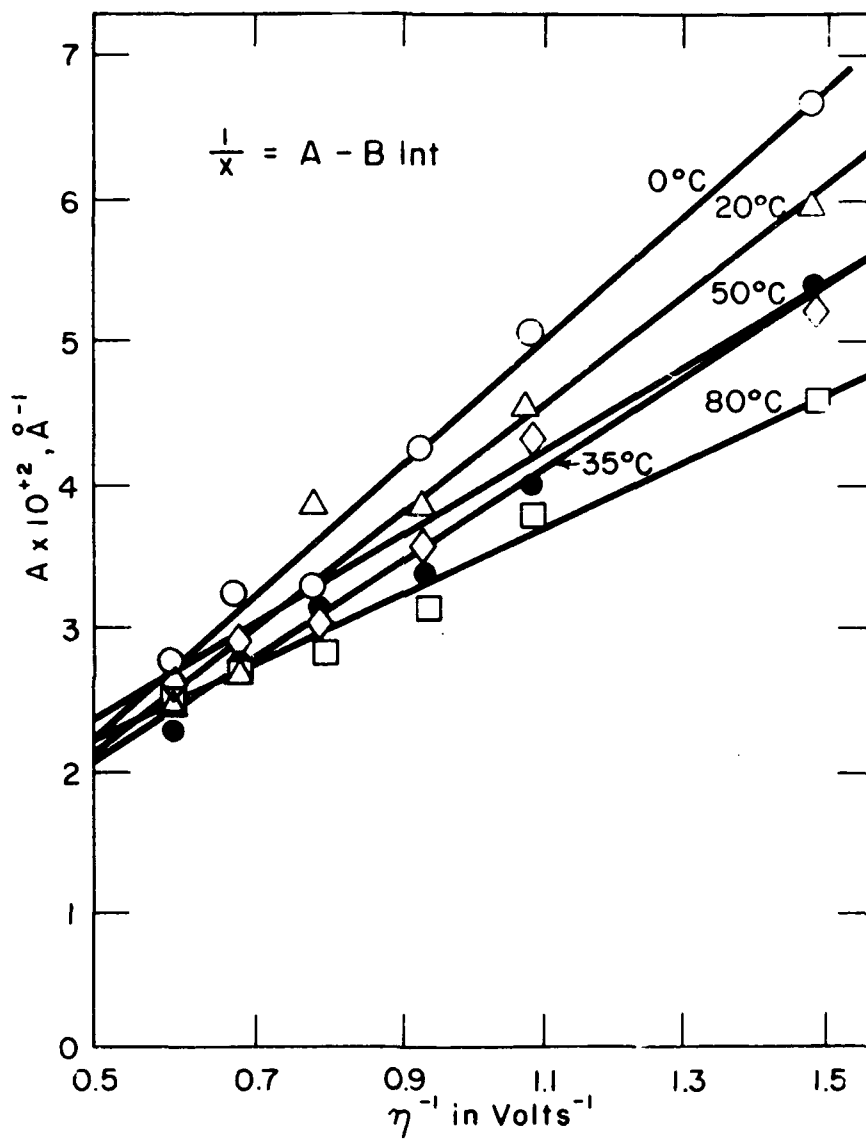


Figure 11. Plots of the rate constant A vs. the reciprocal of the overpotential.

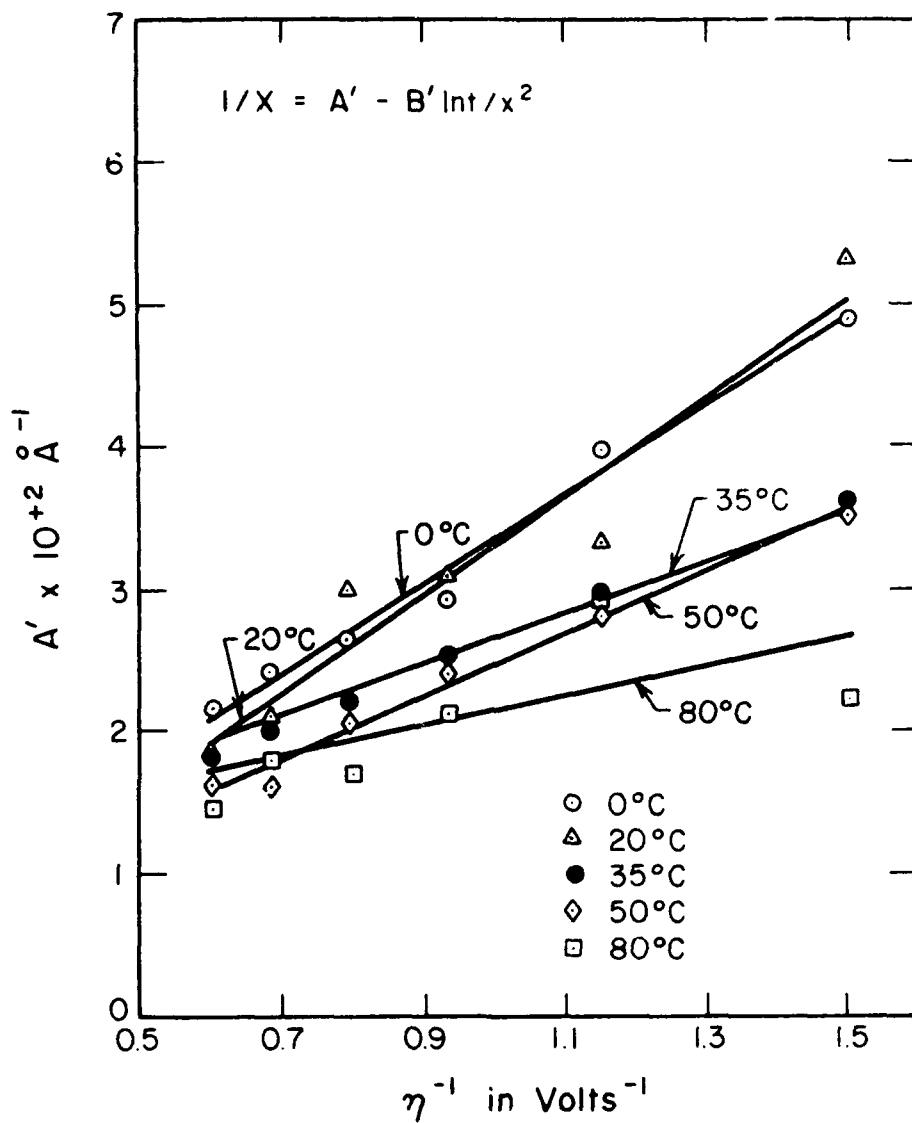


Figure 12. Plots of the rate constant A' vs. the reciprocal of the overpotential.

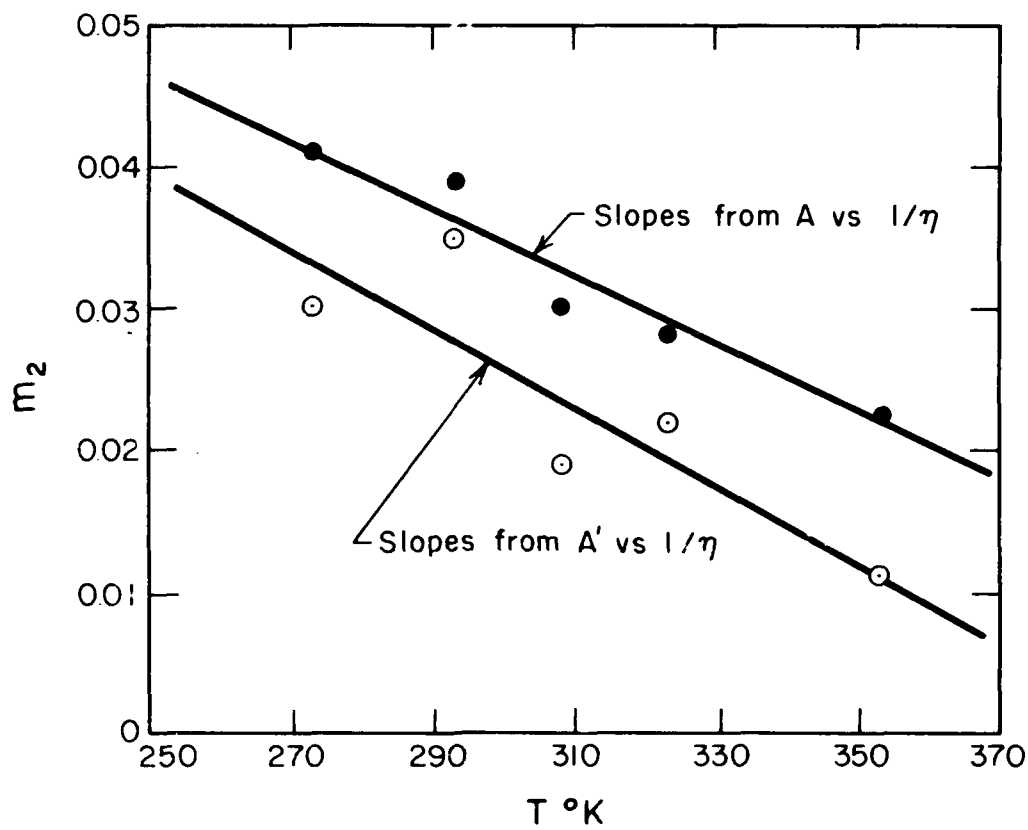


Figure 13. The change in slope with temperature of the A and A' vs. $1/T$ curves.

therefore, it was assumed to be potential independent. The average values are given in Table 3. Figure 14 indicates that D_{av} gives a good linear correlation with temperature. This is in accordance with the constant field model. From the slope the value 9.42×10^8 is obtained for μ .

The Sato-Cohen model gives D as,

$$D = \frac{avRT}{W_0} \quad (11)$$

where W_0 , the activation energy, is split into an enthalpy ΔH_0 and an entropy ΔS_0 term (8, 18)

Thus

$$D = \frac{avRT}{\Delta H_0 - T\Delta S} \quad (12a)$$

or

$$1/D = \frac{\Delta H_0}{avRT} - \frac{\Delta S_0}{avR} \quad (12b)$$

Figure 15 shows that $1/D$ is proportional to $1/T$.

The constant C is proportional to the potential as shown in Figure 16.

From equations 6a and 6b the slopes of Figure 16 are given by

$$m_3 = \frac{avF}{W_0} \quad (13a)$$

or

$$1/m_3 = \frac{\Delta H_0}{avF} - \frac{T\Delta S_0}{avF} \quad (13b)$$

Figure 17 shows that $1/m_3$ is proportional to T in accordance with the Sato-Cohen model. Also from 6a and 6b the intercepts of Figure 16 are a function of temperature;

$$b = \frac{2avRT}{W_0} K, \quad (14a)$$

or

$$1/b = \frac{\Delta H_0}{2savRK} \frac{1}{T} - \frac{\Delta S_0}{2aRK} \quad (14b)$$

Table 3 Constants for the Film Growth Models

mV(SCE)	A (\AA^{-1})	$B \times 10^3$ (\AA^{-1})	A' (\AA^{-1})	B' (\AA^{-1})	C (\AA)	D (\AA)
0°C						
						$D_{av} = 1.04 \text{ \AA}$
-100	0.0668	2.96	0.0492	3.24	11.8	0.82
100	0.0508	1.70	0.0399	1.84	19.5	0.78
300	0.0426	1.38	0.0292	1.81	25.4	1.39
500	0.0325	0.92	0.0265	0.981	30.7	0.89
700	0.0321	1.07	0.0243	1.12	31.0	1.20
900	0.0280	0.826	0.0226	0.895	35.5	1.22
20°C						
						$D_{av} = 1.04$
-100	0.0611	4.12	0.0531	1.31	15.8	1.56
100	0.0450	1.73	0.0334	1.89	22.0	1.00
300	0.0383	1.15	0.0306	1.19	26.1	0.82
500	0.0382	1.21	0.0297	1.30	26.0	0.95
700	0.0271	0.817	0.0210	0.844	37.7	1.26
900	0.0243	0.743	0.0187	0.746	41.0	1.30
35°C						
						$D_{av} = 1.04$
-100	0.0537	2.93	0.0347	3.15	18.3	1.32
100	0.0405	1.57	0.0298	1.62	24.6	1.10
300	0.0340	1.22	0.0252	1.28	29.2	1.25
500	0.0326	1.38	0.0223	1.50	30.3	1.60
700	0.0281	1.01	0.0199	1.20	34.9	1.63
900	0.0249	0.839	0.0183	0.903	39.8	1.60

mV(SCE)	A(Å ⁻¹)	BX10 ³ (Å ⁻¹)	A'(Å ⁻¹)	B'(Å ⁻¹)	C(Å)	D(Å)
50°C						
						$D_{av} = 1.04 \text{ Å}$
-100	0.0514	2.45	0.0352	2.70	19.2	1.16
100	0.0434	2.13	0.0282	2.37	22.8	1.44
300	0.0349	1.51	0.0239	1.63	28.4	1.50
500	0.0302	1.24	0.0206	1.37	32.8	1.68
700	0.0276	1.36	0.0163	1.59	35.9	2.26
900	0.0259	1.15	0.0162	1.34	38.0	2.27
80°C						
						$D_{av} = 1.04$
-100	0.0452	2.86	0.0223	3.17	21.4	2.22
100	0.0373	1.20	0.0294	1.15	26.8	0.93
300	0.0320	1.50	0.0229	1.55	31.0	1.81
500	0.0278	1.47	0.0171	1.45	35.5	2.45
700	0.0270	1.23	0.0178	1.25	36.5	2.13
900	0.0251	1.25	0.0148	1.27	1.26	2.52

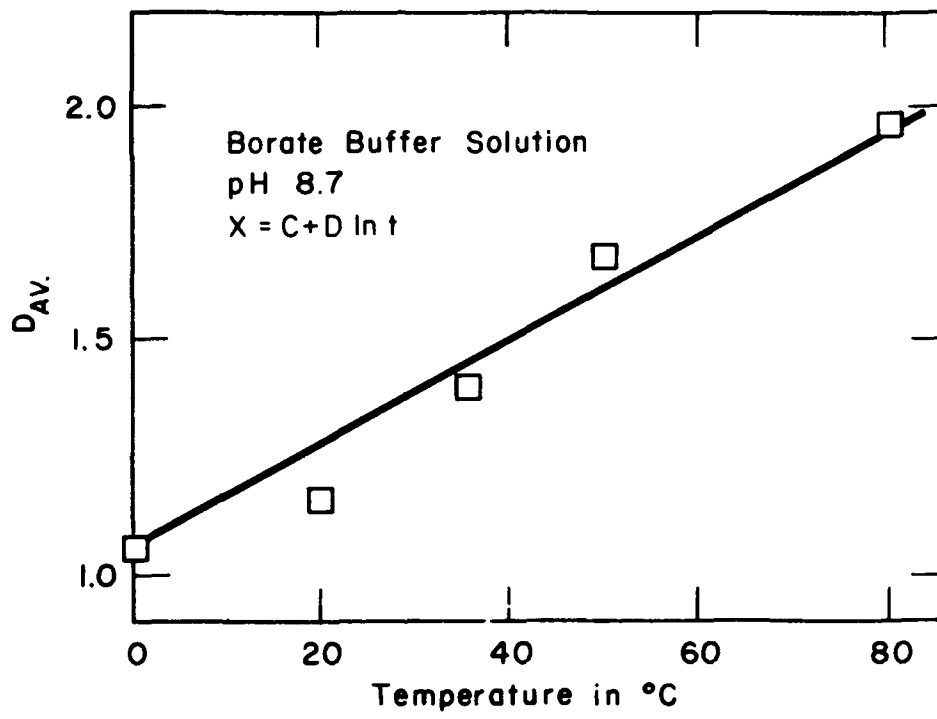


Figure 14. The change in the rate constant D_{AV} with temperature.

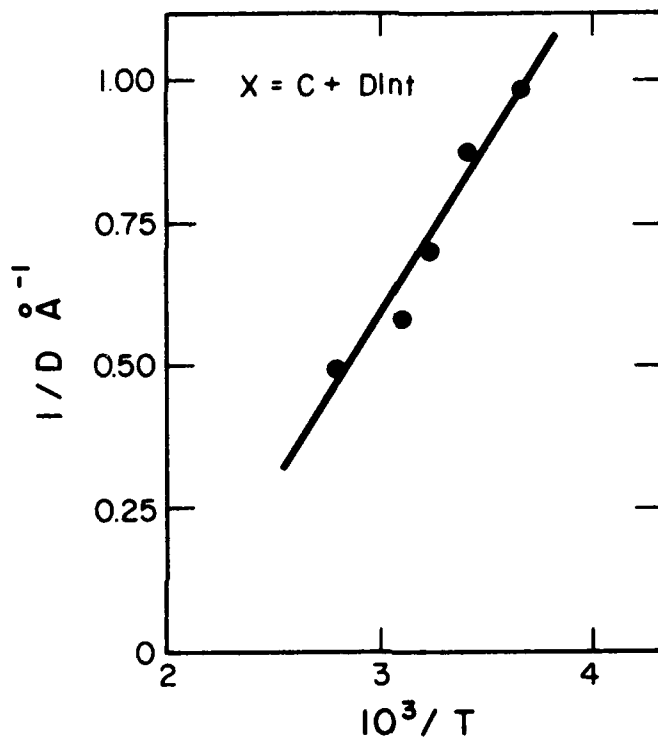


Figure 15. The relationship between the reciprocal of D_{av} and the reciprocal of temperature.

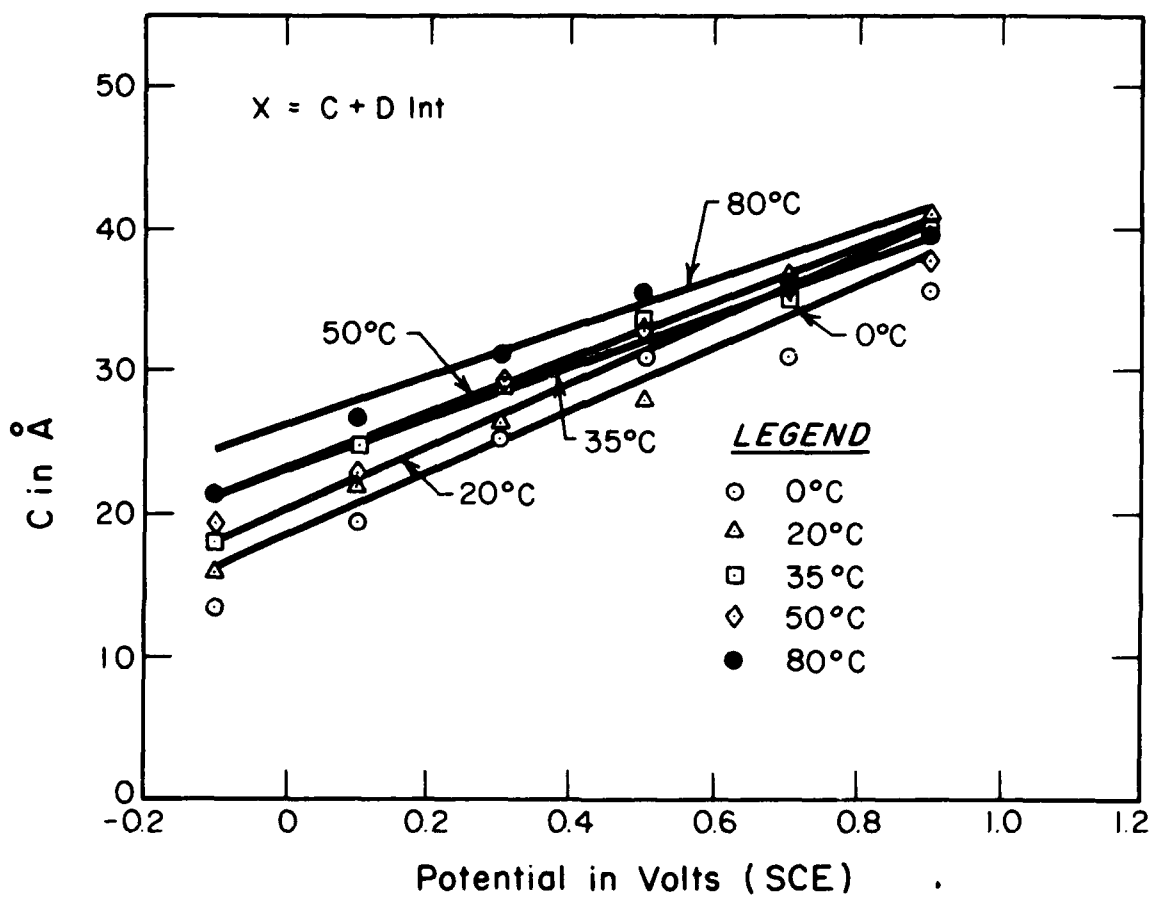


Figure 16. The values of the rate constant C at various applied potentials.

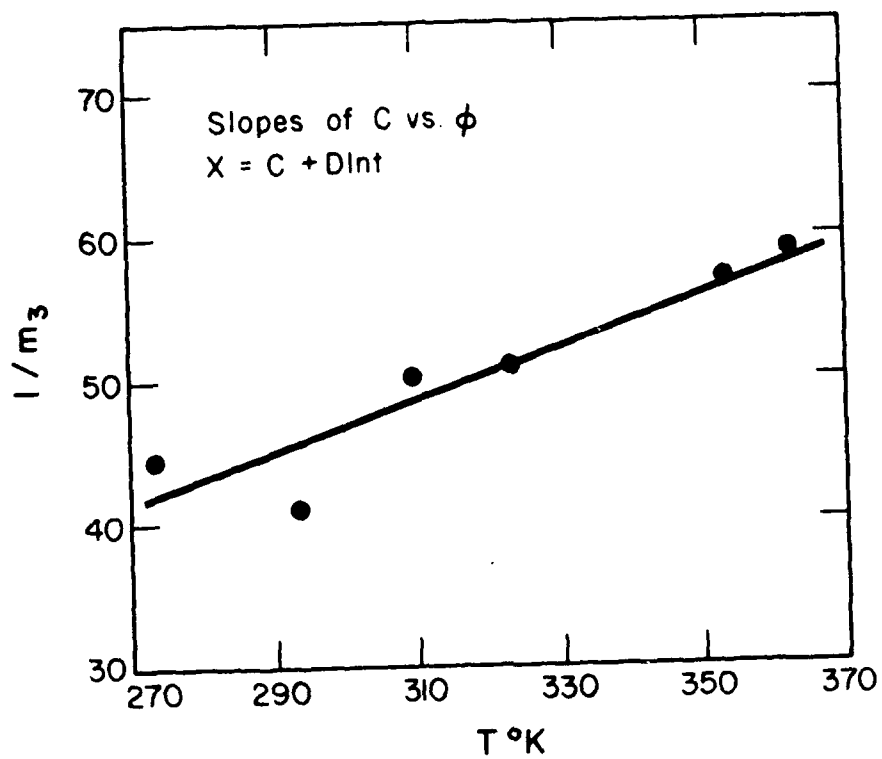


Figure 17. The relationship between the reciprocal of the slopes of the C vs. applied potential curves and temperature.

The intercepts $1/b$ are linearly related to $1/T$ as shown in Figure 18. This assumes that K is a slowly varying function of T .

DISCUSSION

These results have shown that the dual nature of the growth kinetics of passive films on iron observed by others at room temperature (1,4) in borate solutions also apply over the temperature range from the near freezing point to the near boiling point of the solution. In addition, plots of the inverse thickness vs. $\log t/x^2$ also give straight lines over the potential and temperature ranges considered. However, it should be pointed out that it is not possible to determine which type of kinetics is applicable by merely plotting a graph when the film thickness varies over a small range of values. This can be illustrated by eliminating the logarithmic terms of equations 3b and 6b giving

$$\frac{1/A - X}{BX/A} = \frac{C - D}{D} . \quad (15)$$

Thus

$$1/A = C \quad (16)$$

and

$$BX/A = D \quad (17)$$

if the change in X is small. In the same manner it can be shown that

$$B = B' \quad (18)$$

and

$$A = A' - \frac{B}{X} \ln X^2 \quad (19)$$

for small changes in X .

The temperature and potential dependencies of the time independent constants B and B' were found to be consistent with the Mott-Cabrera and

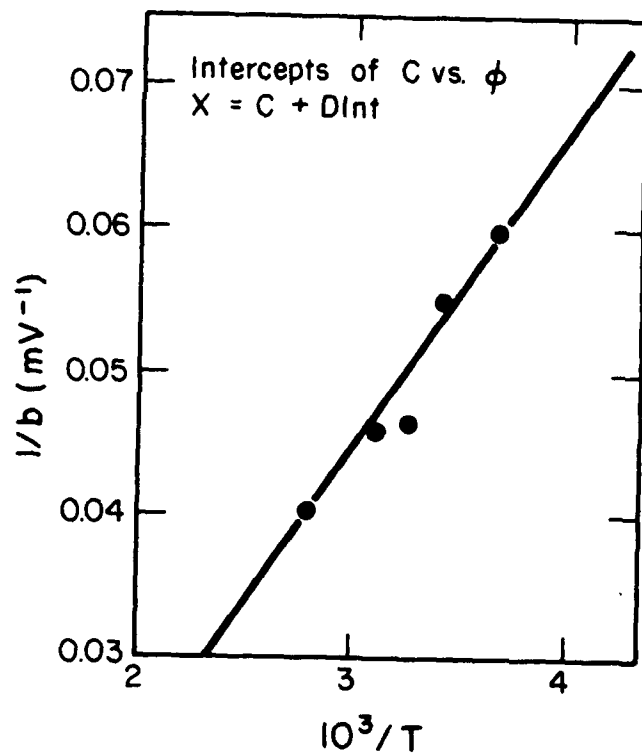


Figure 18. Plot of the intercepts of the curves in Figure 16 vs. the reciprocal of temperature.

modified Mott-Cabrera kinetics respectively, i.e., directly proportional to temperature and inversely proportional to potential. In addition, the jump distance, a , was found to vary linearly with temperature such that

$$a = 25.7 - 0.0633T \quad (20a)$$

in the case of the Mott-Cabrera model and

$$a' = 19.2 - 0.0462T \quad (20b)$$

for the modified Mott-Cabrera model. Thus, expressing a as $a_0 - pT$, the constants B and B' take the form

$$B = B' = \frac{kT}{qaV} = \frac{kT}{8(a_0 - pT)V} + C_1(T) \quad (21)$$

The values for the jump distance, a , are quite large below 100°C. It is difficult to explain these large values within the framework of the assumptions of Mott and Cabrera. Kruger and Calvert have obtained similar values for the jump distance at room temperature (1). They rationalized their results within the Mott-Cabrera model by assuming the film to be composed of two layers with only the outer layer capable of supporting fields of sufficient strength to pull cations across the film. They assumed that the actual value of the jump distance was the product of the apparent value and the fraction of the film which was non-conducting; they estimated that this fraction was approximately 1/3. This assumption and equation 20 lead to the conclusion that the thickness of the dielectric outer layer increases with increase in temperature. However, there still exists an inconsistency since there is a critical temperature at which the jump distance becomes zero. These temperatures are 406°K and 457°K for equations 20a and 20b respectively.

Both the Mott-Cabrera and the modified Mott-Cabrera models give additive constants A and A' respectively which are inversely proportional

to potential across the film and directly proportional to temperature.

However, experimentally

$$A = \frac{1}{n} (10.86 \times 10^{-2} - 2.46T \times 10^{-4}) + C_2 (T) \quad (22a)$$

$$A' = \frac{1}{n} (11.05 \times 10^{-2} - 2.81T \times 10^{-4}) + C'_2 (T) \quad (22b)$$

where the overpotential n has been defined relative to the corrosion potential, -770 mV (SCE). Such a dependence on temperature is not in agreement with the above models. It is interesting to note that there exists a temperature at which A and A' become independent of potential. The temperatures are 441°K and 393°K for A and A' respectively. These temperatures are not far from the critical values found for a and a' .

One can explain the temperature dependent constants in equations 21 and 22, which are the ordinate intercepts in Figures 7, 8, 11, and 12, as resulting from the potential drop across the film being temperature dependent. However, an examination of the intercepts on the potential axis of the $1/B$ vs. ϕ curves suggests that this may not be the complete explanation. These are the potentials at which field dependent growth begins. The values of the intercepts were found to be -498mV, -403mV, -660mV, -1037mV, and -1743mV for 0, 20, 35, 50 and 80°C respectively. Similar values were obtained for the $1/B'$ vs. ϕ curves. It is difficult to rationalize the low values obtained for 50° and 80° since the corrosion potential is -770mV and independent of temperature.

The constant D was found to have a temperature dependence which is consistent with the Sato-Cohen model for film growth. From equation 12b and the least squares equation for the curve in Figure 15, it was found that $\Delta S_0 = 14.8$ cal/deg mole and $\Delta H_0 = 7.19$ k cal/mole; where the lattice constant, a , has been assumed to be 2 Å and v to be 3.

In Figure 16 the constant C was shown to be proportional to the applied potential with a temperature dependent slope, m_3 , in accordance with Sato-Cohen model. The reciprocal of the slopes is proportional to the temperature and related to the enthalpy and entropy as given by equation 13b. Figure 17 shows that $1/m_3$ is proportional to the temperature. The least squares line is

$$1/m_3 = 0.181T - 7.44 \quad (23)$$

The signs are the reverse of those in equation 13b; further, ignoring the signs, the calculated value for the enthalpy is 4310 k cal/mole and that for the entropy is 104 k cal/mole, which are unrealistic numbers.

The activation energies have been determined using the Mott-Cabrera model and are shown in Table 4. The energy W has been determined from the expression given by Mott and Cabrera for the limiting thickness X_L ;

$$X_L = Va'q/(W-39kT) \quad (24)$$

where X_L is the film thickness when the growth rate is 10^{-5} Å/sec. This quantity was calculated by differentiating the expression giving the film growth as a function of time and solving for X when $\frac{dx}{dt} = 10^{-5}$ Å/sec.

The other quantities in this expression are the same as those in equation 1.

The values of W were determined for each temperature using

$$W = 1/p + 39kT \quad (25)$$

where p is the slope of the X_L vs. qaV curve; qaV was determined from the expression

$$qaV = kT/B \quad (26)$$

The values of W, given in Table 4, are approximately the same as those obtained by Kruger and Calvert (1) at room temperature.

From expression 24 there exists a temperature, T_c , such that

$$39 T_c = W \quad (27)$$

above which rapid growth will occur. Using the mean value of W , 2.08 eV, T_c was found to be 620° K.

The activation energy, W' , was determined using (from equation 4a)

$$A' = \frac{kT}{qaV} \ln \frac{kT}{qaVu} = B' \ln B'/u \quad (28)$$

where

$$u = u_0 \exp - (W/kT); \quad (29)$$

therefore, W' can be determined from the slope of the $\ln(u)$ vs. $1/T$ curve. The value of W' was found to be 1.74 eV for 900 mV and 1.63 eV for 300 mV. The average of these two values is 1.68 eV is shown in Table 4.

The activation energy, Q_e , was also calculated using Arrhenius plots of the ellipsometric film thickness after one hour of polarization vs. $1/T$. The values obtained for Q_e at each potential have been plotted against potential in Figure 19. This plot illustrates that Q_e and decreases linearly as the potential is increased or

$$Q_e = W' - mV \quad (30)$$

where V is the potential drop across the film.

Likewise, an activation energy, Q_c , can be determined from an Arrhenius plot of the coulombic film thickness after one hour of polarization vs. $1/T$. This was done for 700 mV by assuming that the passive film was Fe_2O_3 with a density of 5 gm/cm³ and a roughness factor of one. The coulombic film thickness vs. $1/T$ is shown in Figure 20. A value of 2500 cal/mole was obtained; whereas, a value of 500 cal was obtained for Q_e at the same potential. If it is assumed that the difference between the coulombic film thickness and the ellipsometric film thickness is due to film dissolution, then

$$Q_c - Q_e = Q_{diss} \quad (31)$$

Table 4 The jump distances a and a' , the activation energies W and W' of the Mott-Cabrera and the modified Mott-Cabrera models.

Temperature	$^{\circ}\text{K}$	a	a' in Å	W in eV	$W' = 1.68$ eV
273		7.2	6.4	2.16	
293		8.9	6.04	2.11	
308		6.6	5.65	1.84	
323		4.3	3.4	1.80	
353		3.3	3.18	2.50	

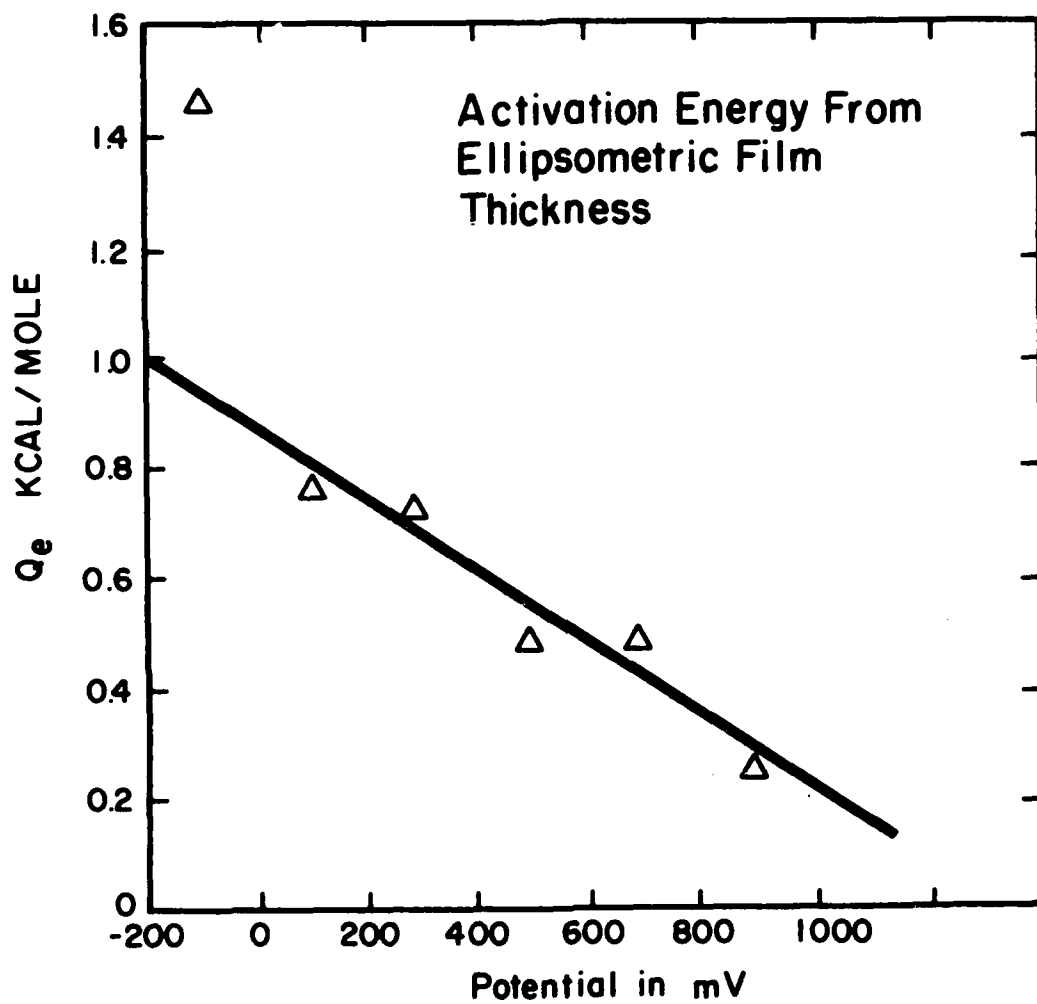


Figure 19. The activation energy determined from the ellipsometric film thickness vs. the applied potential.

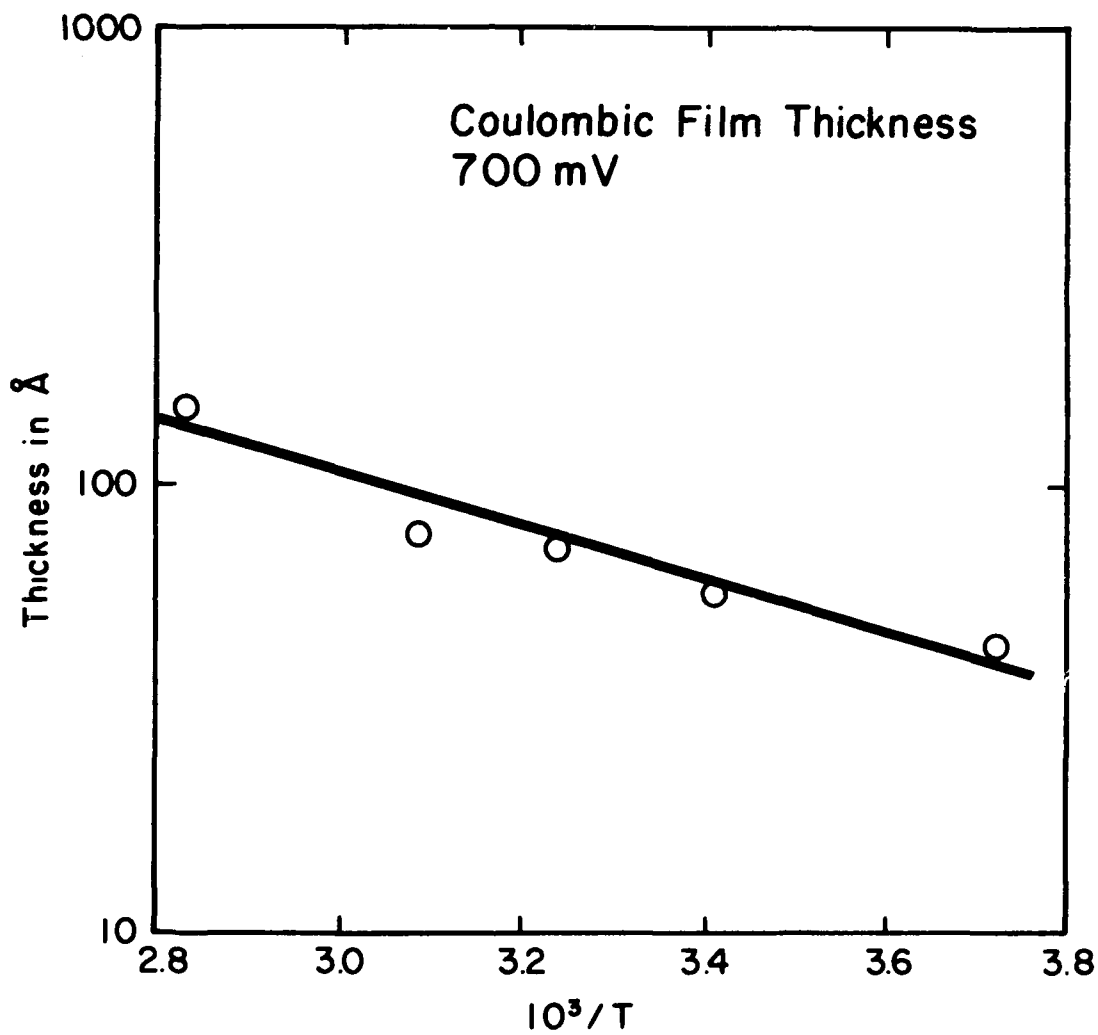


Figure 20. The coulombic film thickness vs. $1/T$.

where Q_{diss} is the activation energy for film dissolution. This gives a value of 2 k cal/mole for Q_{diss} .

In essence it was found that none of the proposed models for passive film growth are completely consistent with the observed temperature and potential effects. The time independent constants A and A' of the two expressions for inverse logarithmic kinetics are inversely proportional to potential in accordance with equations 3a and 4a; however, the temperature dependence is not in accordance with these equations. The constants B and B' of the same kinetic expressions have temperature and potential dependences which are consistent with equations 3a and 4a; but assumptions have to be made in explaining the large value of the jump distances a and a' obtained from these constants. Also, the values obtained for the potentials corresponding to the onset of field dependent growth are difficult to rationalize. The effects of temperature on D of equation 6b were found to be exactly those of the Sato-Cohen model; yet although temperature and potential of dependences C are in accordance with the Sato-Cohen model proportionally, the signs in the functional relationship are not correct physically. Thus either the existing models do not postulate the correct mechanism, or they are in need of modification.

REFERENCES

1. J. Kruger and J. P. Calvert, J. Electrochem. Soc. 110, 670 (1963).
2. J. L. Ord and D. J. DeSmet, ibid., 113, 1258 (1966).
3. N. Sato and K. Kudo, Electrochimica Acta 16, 447 (1971).
4. K. N. Goswami and R. W. Staehle, ibid, 16, 1895 (1971) .
5. F. C. Ho and J. L. Ord, J. Electrochem. Soc. 119, 139 (1972) .
6. J. O'M. Bockris, M. Genshaw, and V. Brusic, Symposium of the Faraday Society, 4, 177 (1970) .
7. H. Wroblowa, V. Brusic, and J. O'M. Bockris, J. Phys. Chem. 75, 2823 (1971) .
8. J. O'M. Bockris, M. A. Genshaw, V. Brusic, and H. Wroblowa, Electrochimica Acta 16, 1859 (1971) .
9. N. Cabrera and N. F. Mott, Rep. Prog. Phys. 12, 163 (1948) .
10. Richard Ghez, J. Chem. Phys. 58, 1838 (1973) .
11. N. Sato and M. Cohen, J. Electrochem. Soc. 111, 512 (1964) .
12. F. P. Fehlner and N. F. Mott, Oxidation of Metals 2, 59 (1970) .
13. H. T. Yolken and J. Kruger, J. Opt. Soc. Am. 55, 842 (1965) .
14. A. B. Winterbottom, J. Iron Steel Inst. 165, 9 (1950) .
15. J. O'M. Bockris, M. A. Genshaw, V. Brusic and W. Wroblowa, Electrochimica Acta 16, 1859 (1971) .
16. G. Bootsma and F. Meyer, Surface Sci. 14, 52 (1969) .
17. F. L. McCrackin and J. P. Colson, NBS Technical Note 242 (1964) .
18. N. Sato, Electrochimica Acta 16, 659 (1971) .